# Chromogranins A and B are key proteins in amine accumulation, but the catecholamine secretory pathway is conserved without them

**Jésica Díaz-Vera,* Marcial Camacho,* José David Machado,* Natalia Domínguez,* Mónica S. Montesinos,* Juan R. Hernández-Fernaud,* Rafael Luján,† and Ricardo Borges*,[1]**

*Unidad de Farmacología, Facultad de Medicina, Universidad de La Laguna, Tenerife, Spain; and †Departamento de Ciencias Médicas, Facultad de Medicina, Universidad de Castilla-La Mancha, Campus Biosanitario, Albacete, Spain

ABSTRACT **Chromogranins are the main soluble proteins in the large dense core secretory vesicles (LDCVs) found in aminergic neurons and chromaffin cells. We recently demonstrated that chromogranins A and B each regulate the concentration of adrenaline in chromaffin granules and its exocytosis. Here we have further studied the role played by these proteins by generating mice lacking both chromogranins. Surprisingly, these animals are both viable and fertile. Although chromogranins are thought to be essential for their biogenesis, LDCVs were evident in these mice. These vesicles do have a somewhat atypical appearance and larger size. Despite their increased size, single-cell amperometry recordings from chromaffin cells showed that the amine content in these vesicles is reduced by half. These data demonstrate that although chromogranins regulate the amine concentration in LDCVs, they are not completely essential, and other proteins unrelated to neurosecretion, such as fibrinogen, might compensate for their loss to ensure that vesicles are generated and the secretory pathway conserved.—Díaz-Vera, J., Camacho, M., Machado, J. D., Domínguez, N., Montesinos, M. S., Hernández-Fernaud, J. R., Luján, R., Borges, R. Chromogranins A and B are key proteins in amine accumulation, but the catecholamine secretory pathway is conserved without them. *FASEB J.* 26, 430–438 (2012). www.fasebj.org**

*Key Words: adrenal · amperometry · chromaffin cells*

Chromogranins (CGs) are the main protein component of the vesicular matrix in many secretory cells (chromaffin, enterochromaffin, pancreatic β-cell, parathyroid, thyroid, and adenohypophysis), as well as in sympathetic and serotonin neurons (for general review see ref. 1). Under low-pH conditions (≈5.5), CGs help to concentrate soluble species in the lumen of secretory vesicles, such as catecholamines (0.5–1 M; refs. 2, 3) or $Ca^{2+}$ (50 mM; refs. 4, 5). Chromogranin A (CgA) is thought to act as a signal for large dense core vesicle (LDCV) biogenesis (6), although exocytosis still occurs in chromaffin cells from $CgA^{-/-}$ mice (3, 7). Indeed, while the lack of CgA does not affect the number of exocytotic events on stimulation, it does reduce the cargo released by chromaffin LDCVs by some 34%, as well as diminish the affinity of catecholamines for the vesicular matrix. Interestingly, the expression of chromogranin B (CgB) increases in the absence of CgA, which probably serves as the sorting signal for the genesis of secretory vesicles when CgA is absent (8, 9). Similarly, in a recently generated $CgB^{-/-}$ mouse strain, we detected a ≈31% reduction in the vesicular amine released and the overexpression of vesicular CgA, with no effect on the exocytotic pathway (10). Chromogranins A and B share some specific characteristics, such as their acidic chains and the presence of an amino-terminal disulfide loop. This terminal loop, present in both CGs, could be a common element for triggering LDCV genesis (9); if this were true, a chromaffin cell lacking both CGs should not have functional LDCVs. However, in a recent report, secretogranin II (the third CG) has been also proposed as a trigger for granulogenesis (11).

In this work, we have combined several techniques to analyze the consequences of the concurrent absence of CgA and CgB. To carry out these experiments, we have produced double $CgA/B^{-/-}$ mutant mice by crossing the $chga^{-/-}/chgb^{+/+}$ and $chgb^{-/-}/chga^{+/+}$ strains. Surprisingly, these mice are viable; furthermore, stimulus-secretion coupling is conserved. Conversely, the analysis of individual exocytotic events revealed a large impairment in the capacity of LDCVs to accumulate catecholamines.

[1] Correspondence: Unidad de Farmacología, Facultad de Medicina, Universidad de La Laguna, E-38071 La Laguna, Tenerife, Spain. E-mail: rborges@ull.es

doi: 10.1096/fj.11-181941

This article includes supplemental data. Please visit *http://www.fasebj.org* to obtain this information.



0892-6638/12/0026-0430 © FASEB

## EXPERIMENTAL PROCEDURES

### Materials

The culture plates were obtained from Nunc (Rochester, NY, USA), the sera were from PAA Laboratories GmbH (Pasching, Austria), and papain was purchased from Worthington (Lakewood, NJ, USA). Culture media and all other drugs were purchased from Sigma-Aldrich (Madrid, Spain), and all the salts used to prepare the buffers were reagent grade. For fibrinogen analyses, we used Santa Cruz Biotechnology (Santa Cruz, CA, USA) antibodies against fibrinogens α, β, and γ (catalog numbers sc-33916, sc-271035, and sc-133156, respectively).

### Animals

The method to generate the $CgA^{-/-}$ and the corresponding wild-type (WT) animals (mice with isogenic background), as well as their phenotype, have been described previously (3, 7). For details of the $CgB^{-/-}$ mice, see refs. 10, 12. We have produced double-mutant $CgA/B^{-/-}$ mice by crossing $chga^{+/-}/chgb^{+/-}$ mice obtained from the mating of the $chga^{-/-}/chgb^{+/+}$ ($CgA^{-/-}$) and $chgb^{-/-}/chga^{+/+}$ ($CgB^{-/-}$) strains, and genotyping the resulting mice by PCR (Supplemental Fig. 2*A*). Three $CgA^{-/-}$ females and 3 $CgB^{-/-}$ males were crossed to obtain F1 mice. Four couples of F1 (hybrids) were then used to produce $CgA/B^{-/-}$ mice (F2) given 1 male and 2 females from a total of 57 animals. To obtain a larger number of double-knockout (KO) mice, we repeated this procedure 3 times and crossed homozygote animals again, getting 5 males and 7 females to establish the colony. We used male animals from F4 to F9 in the present study. All procedures involving animals were performed in accordance with institutional and national guidelines.

### Animal genotyping

Because the CgA-KO mouse was created by deletion of exon 1, and 1.5 kbp of the promoter of the *chga* gene (7) was used for its characterization, 3 primers were used to generate 2 clearly distinguished bands in the same gel. The expected bands were of 2.1 kbp (not shown) and 200 bp (WT), and 400 bp when the *chga* allele was absent (Supplemental Fig. 2*A*): *F-chga*, 5′-CTCCGCCCGCTTCTCT-GCTTTATGCTCGTAG-3′; *R1-chga*, 5′-GTCATGGGGCTGTTCA-CAGGAAGGGCAAAAACTG-3′; *R2-chga*, 5′-GCCCCTAAATGAG-AACCGGCTTCGCG-3′.

As CgB-KO was a homologous recombination of a targeting vector that replaced 117 bases of the proximal promoter region and the first 29 bases of the coding sequence of CgB with the neomycin resistance gene (12), we used only 2 primers for mouse identification. The expected bands were 574 bp (WT) and 1.6 kb in the CgB-KO when the *chgb* allele was disrupted (Supplemental Fig. 2*A*): *F-chgb*, 5′-GAGCCG-GACCCTTGTCCCTTCTTGCC-3′; *R-chgb*, 5′-GCCTGACAT-CTCTGCAGAGAACACAG-3′.

### Cell culture

Chromaffin cells were isolated by papain digestion from the adrenal glands of 1-mo-old mice, as described previously (3, 13).

### Transmission electron microscopy

Mice were heavily anesthetized by intraperitoneal injection of 60 mg/kg pentobarbitone before dissecting out the adrenal glands. This tissue was then fixed overnight by immersion in 2% paraformaldehyde and 2% glutaraldehyde in 0.1 M phosphate buffer (pH 7.4) at 4°C. Subsequently, the tissue was thoroughly washed in phosphate buffer and postfixed in 1% osmium tetroxide for 30 min. After several washes in phosphate buffer, the tissue was treated with 0.1% uranyl acetate, dehydrated in graded ethanol series, and embedded in epoxy resin (Durcupan). Ultrathin sections (70–90 nm) were cut on an ultramicrotome (Reichert Ultracut E; Leica, Austria) and collected on 200-mesh nickel grids. Staining was performed in drops of 1% aqueous uranyl acetate, followed by Reynolds's lead citrate. Ultrastructural analyses were carried out on a Jeol-1010 electron microscope (Jeol Ltd., Akishima, Japan).

### Amperometry and data analysis

The amperometry procedures have been described previously (14). Carbon fiber microelectrodes of a 5-μm radius (Thornel P-55; Amoco Corp., Greenville, SC, USA) were prepared as described previously (15). As the calibration of the microelectrodes was essential to ensure the reproducibility of the results, they were tested by flow-injection analysis. The electrodes were accepted for cell studies when the application of noradrenaline (50 μM) resulted in an oxidation current of 300–400 pA when the solution was run, which should be reduced by 80–100 pA under stop-flow conditions.

Amperometric measurements were obtained using an EPC-10 (Heka Elektronik, Lambrecht/Pfalz, Germany) with the carbon fiber microelectrode gently touching the cell membrane. Cell secretion was stimulated by 5-s pressure injections of 5 mM $Ba^{2+}$ from a micropipette situated 40 μm from the cell. The signals were low-pass-filtered at 1 kHz and collected at 4 kHz. Data were analyzed using locally written macros for IGOR (Wavemetrics, Lake Oswego, OR, USA; ref. 16), and these macros and their user manual can be downloaded (http://webpages.ull.es/users/rborges/).

The analysis of individual exocytotic events included the measurement of the following parameters: $I_{max}$, maximum oxidation current, expressed in picoamperes; $t_{1/2}$, spike width at the half-height, expressed in microseconds; *Q*, spike net charge, expressed in picocoulombs; *m*, ascending slope of spike, expressed in nanoamperes per second (see 16, 17 for details). The recordings were alternated between $CgA/B^{-/-}$ and WT cells on the same day to overcome the variation in electrode sensitivity and secretory responses. We used the average spike values recorded from single cells to estimate 1 statistic/cell (1 cell, $n=1$). The kinetic parameters were calculated as the mean values from ≥20 spikes/cell, and the analyses were achieved by comparing the statistics of WT cells with $CgA/B^{-/-}$ cells (18).

### Intracellular patch electrochemistry

The procedure for electrode and pipette construction has been described previously (19), and whole-cell patch amperometry was adapted from ref. 20. The patch pipette solution contained 140 mM CsOH, 6 mM CsCl, 6 mM HEPES, 0.3 mM Na-GTP, and 2 mM Mg-ATP, adjusted to pH 7.2 with gluconic acid and with an osmolarity of 300–315 mosmol. The procedure for electrode and pipette construction is described elsewhere (3, 19). The baseline was recorded under cell-attached configuration for ≥10 s, and the cell membrane was then broken by suction to analyze the cytosolic amines. (See **Fig. 4*A*** for a drawing of the preparation).

### Whole-cell capacitance

Conventional whole-cell recordings were performed with wax-coated 3–5 MΩ pipettes (Kimax-51; Kimble Products,

Vineland, NY, USA) and an EPC-10 patch clamp amplifier together with the PatchMaster software package (Heka Elektronik). Peak-to-peak sinusoid voltage stimuli of 1000 Hz, 50 mV were superimposed onto a direct current-holding potential of −80 mV. Currents were filtered at 3 kHz and sampled at 10 kHz. To trigger exocytosis a square depolarization pulse was applied from −80 mV (holding potential) to +20 mV during 100 ms. The bathing medium (Krebs-HEPES) contained 5 mM $CaCl_2$.

### Chromaffin granule isolation

Adrenal medullas were triturated using a glass homogenizer in an ice-cold buffer containing 300 mM sucrose, 1 mM EDTA, 1 mM $MgSO_4$, and 10 mM HEPES (pH 7.0), and centrifuged 10 min at 1000 *g* at 4°C. The supernatant was collected and centrifuged at 10,000 *g* for 20 min at 4°C. The resultant pellet was resuspended in an Optiprep (Nycomed Pharma AS, Oslo, Norway) dilution medium containing 300 mM sucrose, 6 mM EDTA, 6 mM $MgSO_4$, and 60 mM HEPES (pH 7) and overlaid on a discontinuous gradient 8/18% OptiPrep. The gradient was made in LoBind tubes (Eppendorf, Hamburg, Germany) to prevent protein loss and centrifuged at 10,000 *g* for 10 h at 4°C. Standard sucrose discontinuous gradient (21) was also used for comparison purposes. The pellet was collected and directly resuspended in 20 μl of denaturing buffer composed of 8 M urea, 4% CHAPS, 40 mM Tris base, 65 mM dithioerythritol, 0.05% SDS, and a trace of bromphenol blue for 2-dimensional analysis. Succinate deshydrogenase was analyzed as described previously (22).

### Western blots

Adrenal medullae were removed and homogenized as described previously (3). Equal amounts of protein extracts (bicinchoninic method) were separated on 10% SDS-polyacrylamide gels, and the proteins were then transferred to polyvinylidene difluoride membranes (PVDF; Hybond-P, Amersham Biosciences, Barcelona, Spain) following a standard protocol. Western blots of adrenal medulla lysates were probed with an anti-secretogranin II (SgII) polyclonal antiserum (raised against a fragment of mouse secretoneurin: a kind gift from Dr. R. Fischer-Colbrie, Innsbruck University, Innsbruck, Austria), diluted 1:3000. Protein bands were visualized by chemiluminescence using an ECL System (GE Healthcare, Little Chalfont, UK), and they were analyzed using a Gel Logic 440 device (Kodak; Rochester, NY, USA) and the accompanying software.

### MALDI-TOF-MS

The procedure for purification of the mouse LDCV fraction has been described previously (10). Isoelectro focusing was performed using glass capillary tubes as described previously (10).

Secretory vesicles purified from 58–66 adrenal glands were required to load 100 μg of total protein onto a single gel, and 2-dimensional gels were stained with colloidal coomassie. Protein spots were manually excised from the stained gels, and the tryptic in-gel digestion and desalting steps were performed using ZipPlates (Millipore, Bedford, MA, USA) according to the manufacturer's instructions. Only differentially expressed proteins were excised and subsequently identified by MS. Mass spectrometery (Bruker-Daltonics, Coventry, UK) was carried out in a positive ion reflection mode, and spectra in the 900-3200 Da range were recorded. The peptide mass fingerprint data were analyzed by the Mascot search engine for protein identification using the Mascot database.

### HPLC analysis of CA

Adrenal medullae were triturated in ice-cold lysis buffer containing perchloric acid (0.05 N), Triton X-100 (0.25%), and dihydroxybenzylamine (100 ng/ml) as the internal standard. The homogenate was centrifuged for 5 min at 10,000 *g*, and the cleared supernatants were injected onto a Shimadzu reverse phase HPLC system (Shimadzu, Kyoto, Japan) with an electrochemical detector (ED), as described previously (23).

### Tyrosine hydroxylase (TH) activity

TH activity from mouse adrenal medullae was measured according to a modified version of a previously published procedure, using saturating concentrations of the natural endogenous pterin cofactor (24) and HPLC, and with electrochemical determination by the conversion of tyrosine to L-dopa.

### Dot-blot analysis

The adrenal medulla homogenates from WT and CgA/B$^{-/-}$ mice were spotted onto PVDF membranes (Immobilon-P; Millipore) using a dot-blot apparatus (Slotblot; GE Healthcare). TH bands were probed with a specific anti-TH mAb (T2928; Sigma), and the dot blots were then reprobed after stripping with an anti-actin polyAb (SC165; Santa Cruz Biotechnology). The TH and actin protein bands were detected by luminescence using the ECL+ system (GE Healthcare), and chemiluminescence signals were detected and analyzed using a VersaDoc imaging system (Bio-Rad Laboratories, Hemel Hempstead, UK).

## RESULTS

### Mouse phenotype and the characterization of adrenal tissues

The animals lacking both CGs did not exhibit any evident differences when compared with WT counterparts in their gross phenotype, locomotor activity, or breeding capacity. Although their weights were normal at birth, an increase in the growth of males was clearly observed in the first 15 wk (Supplemental Fig. S1). The absence of both CGs was confirmed in Western blots, by immunohistochemistry (Supplemental Fig. S2*B, C*) and by 2-dimensional SDS-PAGE (see **Fig. 5** and Supplemental Fig. S3), while both CGs were clearly identified in the corresponding WT control cells from the parental mouse strains (*chga*$^{-/-}$/*chgb*$^{+/+}$ and *chgb*$^{-/-}$/*chga*$^{+/+}$).

Electron microscopy revealed important alterations in the secretory vesicles of the double-KO animals. Secretory vesicles from WT chromaffin cells exhibited a dense core matrix, one-third of the vesicles having a typical half-moon-shaped vesicular matrix (25), and 28 ± 4% of the vesicles were clear (**Fig. 1*A, B***). By contrast, the vesicles from CgA/B$^{-/-}$ mice exhibited a chaotic pattern whereby secretory vesicles were enlarged, with a clear to milky aspect, and with a more dispersed matrix (Fig. 1*C, D*). The vesicle membranes were frequently broken, caused probably by the osmotic stress during the fixation procedure. However,

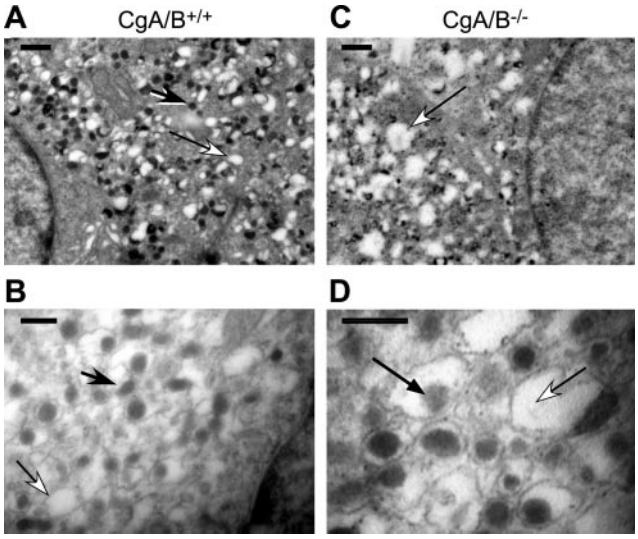


**Figure 1.** Electron micrographs of tissue from WT (CgA/$B^{+/+}$) and double-KO (CgA/$B^{-/-}$) mice. *A*) Black arrow identifies LDCVs typical of mouse adrenomedullary cells; white arrow shows clear vesicles. *B*) Black arrow points to a typical adrenergic granule where some apparently empty vesicles (white arrow) were also observed. *C*) Ultrastructure of CgA/$B^{-/-}$ cells showing clear alterations and the presence of abundant clear giant vesicles (white arrow). *D*) Abundant large clear vesicles (white arrow), some of them with condensed micromatrix (black arrow). Original view: ×20,000 (*A, C*); ×50,000 (*B, D*). Scale bars = 1 μm (*A, C*); 500 nm (*B, D*).

other cell structures, such as the mitochondria, nucleus, or cell membrane, were well conserved in these mutant mice.

In the vesicles obtained from the CgA/$B^{-/-}$ mice, the adrenal catecholamine content was reduced by 54% when measured by HPLC-ED, with norepinephrine falling from 14.2 ± 2.1 to 6.1 ± 1.7 (ng/μg protein, $P$=0.028 *vs.* WT) and epinephrine from 26.5 ± 3.9 to 12.8 ± 1.8 ($P$=0.028 *vs.* WT). By contrast, no changes were observed in the dopamine content ($P$=0.53, Mann-Whitney *U*).

### Secretory studies

Single-cell amperometry on isolated chromaffin cells was used to analyze the single-event secretory characteristics of CgA/$B^{-/-}$ cells. Surprisingly, chromaffin cells lacking CgA and CgB have still triggered exocytosis (**Fig. 2**). However, the cells from the double-KO mice showed a 34% reduction in the number of secretory spikes and a distinct temporal distribution (Fig. 2*C*). This secretion was mediated by a $Ca^{2+}$-dependent exocytosis, as $K^+$-evoked responses were abolished in the absence of external $Ca^{2+}$ (data not shown). The total amount of catecholamines secreted by the CgA/$B^{-/-}$ cells was only 23% of that obtained from control cells (Fig. 2*B*), and this reduction in secretion was due to a 42% decrease in the net catecholamine cargo of individual vesicles (*Q;* see **Table 1**), together with the aforementioned reduction in spike firing. The quantal characteristics also revealed dramatic changes in the kinetics of exocytosis that mainly affected the initial part of the spike.

The secretory response was also quantified by whole-cell capacitance. Despite the large size of LDCVs observed by electron microscopy, we could not resolve individual capacitance jumps. The net increase in cell membrane capacitance was 13.6 ± 2.5 fF for WT ($n$=5) and 12.3 ± 2.15 fF for CgA/$B^{-/-}$ mice ($n$=5, $P$=0.69). A similar increase in membrane addition was observed on stimulation and might be the result of fewer larger exocytotic events of LDCVs. We were not able to obtain reliable secretory recordings using cell attached patch-amperometry from KO cells probably because the distance of the carbon fiber electrode from the cell membrane (≈5 μm) was too large to detect the small amount of amines released by a single quantum event from CgA/B-KO cells. No significant differences in the total $Ca^{2+}$ currents were observed with WT chromaffin cells (−61.5±15.5 pA, $n$=5) and CgA/$B^{-/-}$ (−99.8±26.5 pA, $n$=5).

Despite the availability of cytosolic catecholamines, the uptake of more amines by secretory vesicles from CgA/$B^{-/-}$ chromaffin cells was impaired (**Fig. 3**). As a control experiment, the secretory spikes observed by conventional amperometry showed that incubation with L-dopa produced additional accumulation of catecholamines in the vesicles from WT mice. Indeed, an increase in net charge $Q$ of individual spikes was

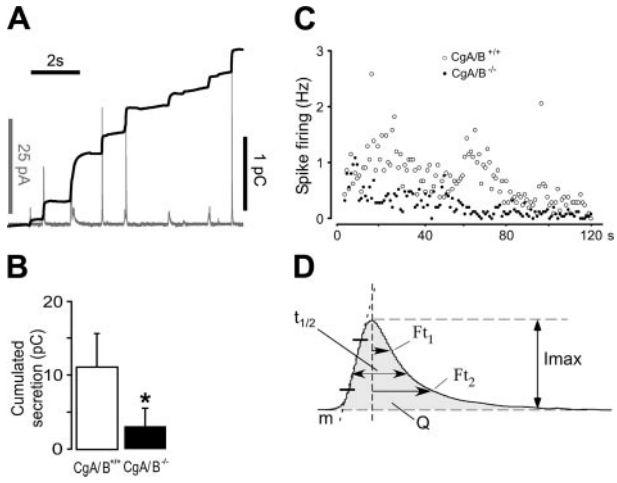


**Figure 2.** Secretory characteristics of chromaffin cells in the absence of chromogranin A and B. Single-cell amperometry was performed with carbon fiber microelectrodes, and exocytosis was elicited by applying a 5-s pulse of $BaCl_2$ (5 mM). *A*) Fragment of an original amperometry recording (gray trace) showing the secretory spikes from a double-KO mouse cell, superimposing the cumulative secretion (black trace). *B*) Pooled secretion from 2-min recordings comparing 12 CgA/$B^{+/+}$ (open bar) with 17 CgA/$B^{-/-}$ cells (solid bar). *$P$ = 0.064; Mann-Whitney *U* test. *C*) Distribution of spike firing frequencies during 2-min amperometric recordings. *D*) Parameters obtained from secretory spikes. Data are quantified in Table 1. $I_{max}$, maximum oxidation current; $t_{1/2}$, spike width at half-height; *Q*, net spike charge; *m*, ascending slope of spike; $Ft_1$ and $Ft_2$, falling times 1 and 2 (time from the maximum point in the spike to reach the $I_{max}/e-1$ and the $I_{max}/e$ of the spike, respectively; see refs. 16, 17 for details). Recordings were alternated between CgA/$B^{-/-}$ and WT cells (18).

TABLE 1. *Kinetic characteristics of individual events in single-cell amperometry of chromaffin cells*

| Cell type | $I_{max}$ (pA) | $Q$ (pC) | $t_{1/2}$ (ms) | $m$ (nA/s) | $Ft_1$ (ms) | $Ft_2$ (ms) | Cells ($n$) |
|---|---|---|---|---|---|---|---|
| CgA/B$^{+/+}$ | 24.5 ± 2.7 | 0.26 ± 0.03 | 9.2 ± 0.4 | 10.17 ± 1.4 | 4.6 ± 0.3 | 8.9 ± 0.5 | 12 |
| CgA/B$^{-/-}$ | 14.3 ± 1.4** | 0.15 ± 0.02** | 9.62 ± 0.8 | 6.1 ± 0.7** | 4.8 ± 0.4 | 9.7 ± 0.9 | 17 |
| Change | −56% | −42% | +5% | −43% | +4% | +9% | |

Data correspond to Fig. 2*D*. Values are means ± SE. **$P < 0.003$; Mann-Whitney $U$ test.

observed by single-cell amperometry. However, when the same experiment was carried out with cells from CgA/B$^{-/-}$ mice, there was no further addition of amines to vesicles, suggesting that their loading capacity was saturated (Fig. 3).

### Intracellular electrochemistry

If the uptake of newly synthesized amines is impaired in secretory vesicles from KO cells, the free cytosolic amines will be highly elevated when the catecholamine precursor L-dopa is applied. Whole-cell patch amperometry was used to measure the free catechols present in the cytosol of chromaffin cells (Fig. 4*A*). Once the cell membrane was broken by suction at the tip of the pipette, there was a sudden increase in the oxidation current (Fig. 4*B*). The signal then dropped exponentially, and a number of spikes were observed in the trace. These spikes could be originated by fusion of the LDCVs with the cell membrane or as a result of vesicles burned to the carbon fiber surface. Nevertheless, we developed a method to rule out the contribution of these spikes to the free catechols detected (10).

The experiments in Fig. 4*C* were performed using the same carbon fiber electrode but on consecutive days, and therefore a direct comparison between basal catechols from WT and KO cells is not accurate. Nevertheless, there was a marked difference in cytosolic free catechols in CgA$^{-/-}$ or CgB$^{-/-}$ chromaffin cell after the incubation with the catecholamine precursor L-dopa. In those mice strains, L-dopa largely increased the levels of catechols in cells from the KO when compared to the WT, whereas the increase of cytosolic catechols caused by L-dopa was similar in WT and CgA/B$^{-/-}$ (Fig. 4*C* and refs. 3, 10, 26).

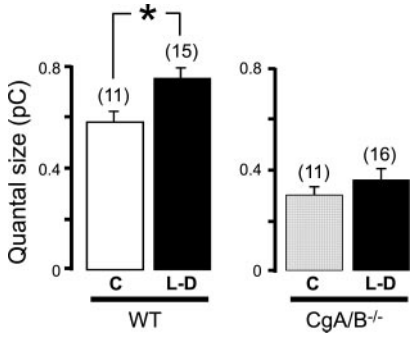


**Figure 3.** Effects of L-dopa overload on LDCV content. Intact single chromaffin cells were incubated in the presence or in the absence of L-dopa (100 μM, 90 min, L-D) and the secretion was analyzed using conventional amperometry $BaCl_2$ (5 mM) was used as secretagogue, and the secretory response was monitored for 2 min. Bars show the net catecholamine content of vesicles ($Q$) of chromaffin cells from WT and CgA/B$^{-/-}$ mice (means±SE). A statistical comparison between cells from WT and CgA/B$^{-/-}$ mice is not possible because the experiments were performed on different days. *$P < 0.05$; Mann Whitney $U$ test.

### TH

The overall activity of TH in adrenomedullary tissues was 65% greater in the CgA/B-KO than in the WT and in Western blots; this increase appeared to be mostly caused by the overexpression of TH (Supplemental Fig. S2) and not by an activation of the enzyme (**Table 2**).

### Characterization of vesicular proteins

Since the lack of CgA promotes the overexpression of CgB and *vice versa*, it was notable that the absence of both granins did not significantly increase the expression of SgII (an additional member of the family) in adrenomedullary tissues (Supplemental Fig. S2*C*, *D*). A proteomic analysis unexpectedly revealed the presence of large amounts of fibrinogen, as well as heat-shock proteins, in isolated chromaffin vesicles, while the α, β, and γ monomers of fibrinogen were not found in any gel from WT mice (**Table 3**, Fig. 5, and Supplemental Fig. S3).

## DISCUSSION

We have produced double-mutant CgA/B$^{-/-}$ mice by crossing CgA$^{-/-}$ (7) and CgB$^{-/-}$ (12) strains. The proportion of CgA/B$^{-/-}$ mice obtained from the cross of heterocygotes (chga$^{+/-}$/chgb$^{+/-}$ mice) was similar (≈6.1%) to that expected from mendelian distribution (6.25%). Animals did not contain detectable amounts of these CGs, but they were viable and fertile, with no gross phenotype differences with their heterozygote or WT counterparts. However, electron microscopy revealed important alterations in the secretory vesicles of the double-KO animals. Indeed, secretory vesicles from WT chromaffin cells exhibited the typical dense core matrix (25) in electron micrographs (shown in Fig. 1*A*, *B*). By contrast, the vesicles from CgA/B$^{-/-}$ mice exhibited a chaotic pattern whereby secretory vesicles were enlarged, with a clear to milky aspect and a more dispersed matrix observed in electron microscopy (Fig.

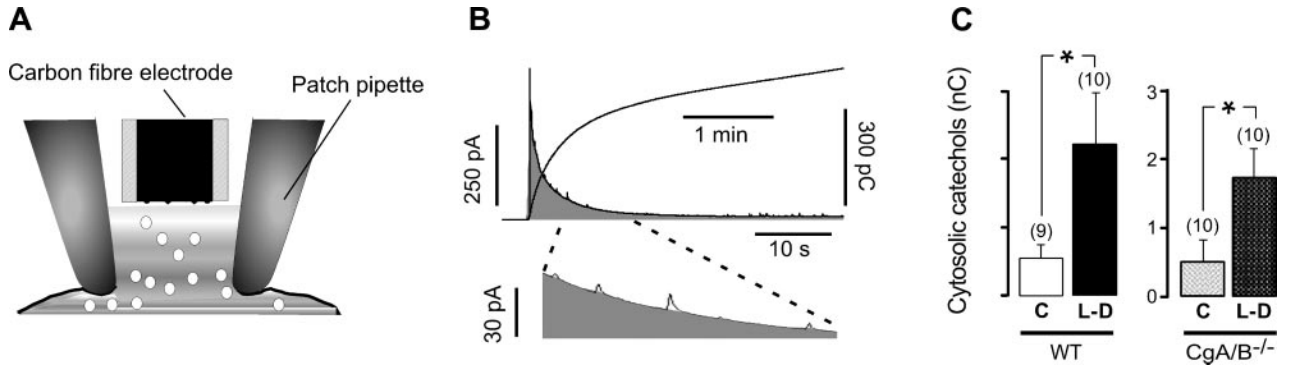


**Figure 4.** Effects of L-dopa overload on free cytosolic catechols. All cells were incubated with 10 μM pargyline for preventing degradation by MAO. Number of cells utilized in these studies is displayed in brackets. *A*) Drawing shows how an individual cell was observed using patch-amperometry in the whole-cell configuration mode, and how the cytosol was brought into contact with the carbon fiber electrode by aspiration. *B*) Top recording shows the oxidation trace obtained after breaking the cell membrane (scale in picoamperes). Integral of the amperometric trace is overlapped (scale in picocoulombs). To obtain the integrated recording, a macro written locally for Igor Pro was used to eliminate the contribution of spikes that overlapped the recording due to the net free cytosolic amines, as shown in the bottom trace. *C*) Bars show pooled data (expressed in nanocoulombs) from 120-s integration of the oxidation current obtained under basal conditions (C) and after treatment with L-dopa (100 μM, 90 min, L-D) of cells from WT and CgA/B$^{-/-}$ mice. Note that this panel is divided into 2 graphs, as the WT and CgA/B$^{-/-}$ experiments were conducted on different days using different electrodes. Number of cells is indicated in parentheses. *$P <$ 0.016; Mann-Whitney *U* test with Bonferroni correction, $\alpha = 0.012$.

1*C, D*). The vesicular membranes were fragile and frequently were damaged during the fixation procedure; this was caused probably by the osmotic changes occurring during glutaraldehyde incubation. Careful observation of electron microscopy images already published from chromaffin cells lacking CgA identified similarly distorted vesicles (27, 28), though the changes were not as dramatic as those found in these double mutants. As secretory vesicles behave as "perfect osmometers" that shrink or swell according to the external tonicity (29), it is likely that vesicles lacking CGs are labile to osmotic stress and their ability to concentrate catecholamines is impaired.

The HPLC analyses revealed a significant reduction in the cell content of catecholamines. It is noteworthy that catecholamines are mostly restricted to LDCVs in chromaffin cells, and only a small fraction can be found free in the cytosol (≈50 μM; ref. 20) compared to the higher values of 800 mM in LDCVs (3). As LDCVs occupy an important fraction (≈20%) of the cell, it can be concluded that HPLC assayed the average amount of catecholamines in the whole population of LDCVs.

We can summarize the kinetics of exocytosis in CgA/B$^{-/-}$ chromaffin cells when compared to that in CgA$^{-/-}$ and CgB$^{-/-}$ as follows: the lack of CgA in CgA-KO animals is partially compensated by overexpression of CgB, where the amine cargo in these cells is decreased by 34%. In addition, it appears that CgB cannot retain amines as efficiently as CgA, accelerating exocytosis. The lack of CgB in CgB-KO animals results in a similar decrease in amine content (31%), yet exocytosis is slower, since CgA binds amine with higher affinity. The lack of both amines produces a large decrease in amine content (42%) in large vesicles, which slows exocytosis. Although both CGs have been proposed as proteins capable of generating secretory vesicles for exocytosis (6, 30), chromaffin cells lacking chromogranins A and B are able to undergo triggered exocytosis, as evident from the secretory pattern observed in these cells (Fig. 2). However, the cells from the double-KO mice showed a significant reduction in the number of secretory spikes as well as a different temporal distribution (Fig. 2*C*). This reduction could reflect the presence of fewer vesicles at the cell membrane, caused by a restriction in their movement toward the exocytotic sites (due to their large size) or deficiencies in the stimulus-secretion coupling processes. The total amount of catecholamines secreted by the CgA/B$^{-/-}$ cells was dramatically reduced (Fig. 2*B*), and this reduction in secretion was largely due to the decrease in the net catecholamine cargo of individual vesicles (Table 1). The quantum characteristics also revealed dramatic changes in the kinetics of exocytosis that mainly affected the initial part of the release

TABLE 2. *TH activity and expression in the WT and CgA/B-KO adrenal medulla*

| Cell type | TH activity (nmol/mg protein/min) | TH content (blot density) | TH activity/blot ratio |
|---|---|---|---|
| WT | 4.5 ± 0.7 | 2.73 ± 0.7 | 1.64 |
| CgA/B$^{-/-}$ | 7.5 ± 1.3* | 4.31 ± 0.9* | 1.74 |
| Change | ~65% | ~58% | NS |

TH activity was measured *in vitro* by HPLC. TH content was obtained in dot-blots and referenced as the product of the mean image density. All data are means ± SE of 10 WT and 7 CgA/B$^{-/-}$ mice. NS, nonsignificant. *$P < 0.05$; Mann-Whitney *U* test.

TABLE 3. *Proteins present in the LDCV of chromaffin cells identified by MALDI-TOF-MS*

| Spot | Protein | NCBI no. (gi) | MW (Da) | pI | Matched peptides | Sequence coverage (%) | Mascot score | Missed cleavage | CgA/B$^{-/-}$ fold change |
|---|---|---|---|---|---|---|---|---|---|
| 1 | Chromogranin B | 50403 | 78,036 | 5.01 | 11 | 20 | 113 | 1 | Only in WT |
| 2 | Secretogranin 2, precursor | 417771 | 70,600 | 4.69 | 18 | 31 | 194 | 2 | +1.65 |
| 3 | Chromogranin A | 26338173 | 51,929 | 4.65 | 8 | 15 | 66 | 3 | Only in WT |
| 4 | Discs, large homologue 2 (*Drosophila*)/ chapsin 110 | 26338173 | 54,421 | 6.93 | 6 | 18 | 68 | 1 | Only in WT |
| 5 | Inter α-trypsin inhibitor, heavy chain 4 | 12836422 | 100,375 | 6.13 | 10 | 13 | 79 | 1 | Only in KO |
| 6 | Heat shock protein 90, β (Grp94), member 1 | 309220 | 92,703 | 4.74 | 15 | 20 | 65 | 1 | Only in KO |
| 7 | Prolyl 4-hydroxylase, β polypeptide/ protein disulfide isomerase-precursor | 14250251 | 57,442 | 4.77 | 15 | 34 | 137 | 2 | Only in KO |
| 8 | Fibrinogen γ chain | 18043449 | 50,044 | 5.54 | 18 | 37 | 137 | 2 | Only in KO |
| 9 | Fibrinogen β chain | 21619364 | 55,402 | 6.68 | 10 | 23 | 100 | 1 | Only in KO |
| 10 | Fibrinogen α chain | 13529485 | 61,801 | 7.16 | 23 | 33 | 175 | 2 | Only in KO |
| 11 | Acyl-coenzyme A dehydrogenase, short chain | 16740777 | 45,146 | 8.68 | 7 | 25 | 63 | 1 | Only in KO |
| 12 | Apolipoprotein E | 192005 | 35901 | 5.56 | 12 | 51 | 94 | 2 | Only in KO |
| 13 | Dihydrolipolylysine residue succinyltransferase component of 2 oxoglutarate dehydrogenase complex | 62510833 | 49306 | 9.11 | 8 | 16 | 56 | 2 | Only in WT |

Numbers correspond to spots excised from gels such as that shown in Fig. 5.

(rising part of the spike). These changes were similar to those observed in the CgB-KO animals where the ascending part of the amperometric spikes were slower (10), although they were opposite to those seen in the CgA-KO where the descending part of the amperometric spikes was strongly accelerated (3). Large vesicles released at low frequency could explain why whole-cell capacitance recordings did not show quantitative differences between CgA/B-KO and WT cells.

The experiments summarized in Fig. 3 suggest that secretory vesicles from CgA/B-KO cells cannot uptake more amines despite newly available catecholamines after the incubation with L-dopa (Fig. 4*C*). It was similar to that found with chromaffin cells from CgA- (3) and CgB-KO mice (10, 26), and it seems that the loading capacity of vesicles was saturated. Alternatively, VMAT expression may be reduced, although there was no evidence of this in Western blots (data not shown).

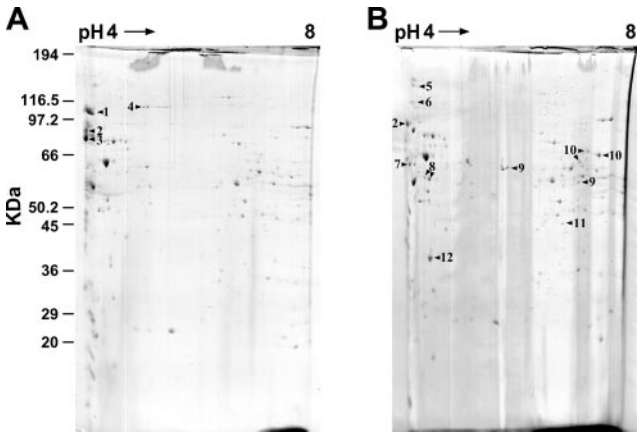


**Figure 5.** Bidimensional gel electrophoresis of the cell fraction enriched in vesicles from WT and CgA/B$^{-/-}$ mice. A total 100 μg of protein was separated by 2-dimensional electrophoresis and stained with colloidal coomassie blue ProtoBlue. A representative gel is shown; proteins indicated by arrowheads are listed in Table 3. Molecular mass markers and pH values are indicated.

The limiting step in catecholamine synthesis is the enzyme that converts the amino acid tyrosine into L-dopa. The overall activity of TH was greater in CgA/B-KO medullas than in WT, an increase that seems to be caused by the overexpression of TH (Supplemental Fig. S2). These data, together with the lower levels of cytosolic catechols, indicate that despite their higher synthetic capacity, vesicle catecholamine levels cannot be higher. Furthermore, the increase in cytosolic amines produced by incubation with L-dopa also failed to introduce more catecholamines into LDCVs (Fig. 3). The levels of TH mRNA are higher in the adrenomedullary tissues of the CgA-KO (7, 28), although there was no significant increase in the expression of this enzyme in the CgA-KO (3) or the CgB-KO (10). The overexpression of TH found in the double KO probably reflects the effort to maintain a maximal concentration of vesicular amines. The relatively lower ability of the LDCVs to take up more amines and the low levels of cytosolic catechols found means that catabolism is also apparently accelerated.

Based on experiments where CgA (6) or CgB (8) are expressed, it appears that both CGs are important for the biogenesis of LDCVs. Also, it has been claimed that the highly conserved disulfide bonded loop corresponding to exons I and II at the N terminus of the CgA gene is essential for LDCV sorting (9, 31). However, in our experiments, the occurrence of exocytotic release indicates that the presence of CGs is not the sole

requirement to promote LDCV genesis or to maintain the secretory machinery functional.

The lack of CgA promotes the overexpression of CgB and *vice versa* (26). Conversely, the absence of both granins did not significantly increase the expression of SgII (Supplemental Fig. S5*C, D*). Which other proteins could be taking some of the roles of CGs? The proteomic analysis of isolated chromaffin vesicles of KO cells did not show the overexpression of other granins but unexpectedly revealed the presence of large amounts of α, β, and γ monomers of fibrinogen, as well as heat-shock proteins (Table 3). Conversely, fibrinogen was absent in vesicles from WT animals (Fig. 5 and Supplemental Fig. S3). This fibrinogen expression may be especially relevant, as it shares some features with CgA and B, such as the ability to bind $Ca^{2+}$ and catecholamines (32, 33). Also, fibrinogens have been proposed to control the genesis of secretory vesicles (34, 35) as they contain amino-terminal loops. It is possible that fibrinogens could help to compensate for the lack of CGs in secretory vesicle and facilitate SgII-induced biogenesis or their sorting. However, the capacity of the soluble proteins overexpressed in the LDCVs seems insufficient to maintain their structure and function intact (Fig. 5). As another possible means of confirming that the fibrinogen is localized in the secretory granules, we attempted to detect the fibrinogen secreted from cultured chromaffin cells and adrenal slices, after stimulation with depolarizing solutions (isotonic KCl 60 mM, for 30 s). We used antibodies against the 3 subunits for detection by inmmunocytochemistry, trying to detect fluorescent patches on the membranes of intact cells, but this was unsuccessful, probably because of the sensitivity of the antibodies or the minute amounts of fibrinogen.

We also attempted to demonstrate the exocytosis of fibrinogens from mouse adrenal slices after the same stimulation, again with little success, probably because of the minute amounts of proteins released or their retention within the vesicle. The presence of the weak matrix observed in EM images might be the result of the aggregation of intravesicular proteins after cross-linking with glutaraldehyde. However, the short life span of primary mouse chromaffin cells in culture complicates the use of silencing techniques to study the function of intravesicular proteins like fibrinogens or SgII. Ideally, immunoelectron microscopy would detect the presence of SgII and fibrinogen inside secretory vesicles. However, we failed, probably because these antibodies were interfered by the fixation procedure and because gold particles can penetrate only a few micrometers of the tissues.

Taken together, our data show that homozygous $CgA/B^{-/-}$ mice are viable and fertile, and that they are still capable of generating secretory vesicles for exocytosis. However, the vesicles generated in chromaffin cells from these mice are very large with a small matrix, and their capacity to concentrate catecholamines is largely impaired. Our results support the essential role of CGs in the storage and exocytosis of biological amines, although it seems that in their absence, SgII (11) and perhaps other proteins, such as fibrinogens, might fulfill their role in secretory vesicle biogenesis. FJ

J.D.V. and N.D. are the recipients of a FPU fellowship from the Spanish Ministry of Science and Innovation (MICINN). J.D.M. holds a Consolider contract (CSD2008-00005). This work was supported by the Spanish Ministry of Science and Innovation (BFU2010-15822) and Consolider (R.B.), and the Canary Islands Agency for Research, Innovation and Information Society PI2007/017 (J.D.M.). The authors are grateful to Daniel O'Connor and Sushil Mahata (University of California, San Diego, CA, USA) for providing the $CgA^{-/-}$ mice, and to Wieland Huttner and Federico Callegari (Max Planck Institute of Molecular Biology and Genetics, Dresden, Germany) for providing the $CgB^{-/-}$ mice. Agustin Castañeyra and Emilia Carmona helped to obtain the immunocytochemistry images. The authors also thank the personnel of the animal house of the University of La Laguna for maintaining the mouse strains. Discussions with Humberto Viveros, Lucio Díaz-Flores, Reiner Fischer-Colbrie, and Mark Sefton were whole-heartedly appreciated. The authors declare no conflicts of interest.

## REFERENCES

1. Helle, K. B. (2000) The chromogranins. Historical perspectives. *Adv. Exp. Med. Biol.* **482,** 3–20
2. Finnegan, J. M., Pihel, K., Cahill, P. S., Huang, L., Zerby, S. E., Ewing, A. G., Kennedy, R. T., and Wightman, R. M. (1996) Vesicular quantal size measured by amperometry at chromaffin, mast, pheochromocytoma, and pancreatic beta-cells. *J. Neurochem.* **66,** 1914–1923
3. Montesinos, M. S., Machado, J. D., Camacho, M., Diaz, J., Morales, Y. G., Alvarez de la Rosa, D., Carmona, E., Castaneyra, A., Viveros, O. H., O'Connor, D. T., Mahata, S. K., and Borges, R. (2008) The crucial role of chromogranins in storage and exocytosis revealed using chromaffin cells from chromogranin A null mouse. *J. Neurosci.* **28,** 3350–3358
4. Winkler, H., and Westhead, E. (1980) The molecular organization of adrenal chromaffin granules. *Neuroscience* **5,** 1803–1823
5. Santodomingo, J., Vay, L., Camacho, M., Hernandez-Sanmiguel, E., Fonteriz, R. I., Lobaton, C. D., Montero, M., Moreno, A., and Alvarez, J. (2008) Calcium dynamics in bovine adrenal medulla chromaffin cell secretory granules. *Eur. J. Neurosci.* **28,** 1265–1274
6. Kim, T., Tao-Cheng, J. H., Eiden, L. E., and Loh, Y. P. (2001) Chromogranin A, an "on/off" switch controlling dense-core secretory granule biogenesis. *Cell* **106,** 499–509
7. Mahapatra, N. R., O'Connor, D. T., Vaingankar, S. M., Hikim, A. P., Mahata, M., Ray, S., Staite, E., Wu, H., Gu, Y., Dalton, N., Kennedy, B. P., Ziegler, M. G., Ross, J., and Mahata, S. K. (2005) Hypertension from targeted ablation of chromogranin A can be rescued by the human ortholog. *J. Clin. Invest.* **115,** 1942–1952
8. Huh, Y. H., Jeon, S. H., and Yoo, S. H. (2003) Chromogranin B-induced secretory granule biogenesis: comparison with the similar role of chromogranin A. *J. Biol. Chem.* **278,** 40581–40589
9. Glombik, M. M., Kromer, A., Salm, T., Huttner, W. B., and Gerdes, H. H. (1999) The disulfide-bonded loop of chromogranin B mediates membrane binding and directs sorting from the trans-Golgi network to secretory granules. *EMBO J.* **18,** 1059–1070
10. Diaz-Vera, J., Morales, Y. G., Hernandez-Fernaud, J. R., Camacho, M., Montesinos, M. S., Calegari, F., Huttner, W. B., Borges, R., and Machado, J. D. (2010) Chromogranin B gene ablation reduces the catecholamine cargo and decelerates exocytosis in chromaffin secretory vesicles. *J. Neurosci.* **30,** 950–957
11. Courel, M., Soler-Jover, A., Rodriguez-Flores, J. L., Mahata, S. K., Elias, S., Montero-Hadjadje, M., Anouar, Y., Giuly, R. J., O'Connor, D. T., and Taupenot, L. (2010) Pro-hormone

secretogranin II regulates dense core secretory granule biogenesis in catecholaminergic cells. *J. Biol. Chem.* **285,** 10030–10043
12. Obermuller, S., Calegari, F., King, A., Lindqvist, A., Lundquist, I., Salehi, A., Francolini, M., Rosa, P., Rorsman, P., Huttner, W. B., and Barg, S. (2010) Defective secretion of islet hormones in chromogranin-B deficient mice. *PLoS ONE* **5,** e8936
13. Sorensen, J. B., Nagy, G., Varoqueaux, F., Nehring, R. B., Brose, N., Wilson, M. C., and Neher, E. (2003) Differential control of the releasable vesicle pools by SNAP-25 splice variants and SNAP-23. *Cell* **114,** 75–86
14. Machado, J. D., Montesinos, MS., and Borges, R. (2008) Good practices in single cell amperometry. In *Exocytosis and Endocytosis: Methods in Molecular Biology*, Vol. 440 (Ivanov, A. I., ed) pp. 297–313, Humana Press, Totowa, NJ, USA
15. Kawagoe, K. T., Zimmerman, J. B., and Wightman, R. M. (1993) Principles of voltammetry and microelectrode surface states. *J. Neurosci. Methods* **48,** 225–240
16. Segura, F., Brioso, M. A., Gomez, J. F., Machado, J. D., and Borges, R. (2000) Automatic analysis for amperometrical recordings of exocytosis. *J. Neurosci. Methods* **103,** 151–156
17. Machado, J. D., Segura, F., Brioso, M. A., and Borges, R. (2000) Nitric oxide modulates a late step of exocytosis. *J. Biol. Chem.* **275,** 20274–20279
18. Colliver, T. L., Hess, E. J., and Ewing, A. G. (2001) Amperometric analysis of exocytosis at chromaffin cells from genetically distinct mice. *J. Neurosci. Methods* **105,** 95–103
19. Dernick, G., Gong, L. W., Tabares, L., Alvarez de Toledo, G., and Lindau, M. (2005) Patch amperometry: high-resolution measurements of single-vesicle fusion and release. *Nat. Methods* **2,** 699–708
20. Mosharov, E. V., Gong, L. W., Khanna, B., Sulzer, D., and Lindau, M. (2003) Intracellular patch electrochemistry: regulation of cytosolic catecholamines in chromaffin cells. *J. Neurosci.* **23,** 5835–5845
21. Smith, A. D., and Winkler, H. (1967) A simple method for the isolation of adrenal chromaffin granules on a large scale. *Biochem. J.* **103,** 480–482
22. Munujos, P., Collcanti, J., Gonzalez-Sastre, F., and Gella, F. J. (1993) Assay of succinate dehydrogenase activity by a colorimetric-continuous method using iodonitrotetrazolium chloride as electron acceptor. *Anal. Biochem.* **212,** 506–509
23. Borges, R., Sala, F., and Garcia, A. G. (1986) Continuous monitoring of catecholamine release from perfused cat adrenals. *J. Neurosci. Methods* **16,** 289–300
24. Nagatsu, T., Oka, K., Numata, Y., and Kato, T. (1979) A simple and sensitive fluorescence assay for tyrosine hydroxylase activity. *Anal. Biochem.* **93,** 82–87
25. Crivellato, E., Nico, B., Perissin, L., and Ribatti, D. (2003) Ultrastructural morphology of adrenal chromaffin cells indicative of a process of piecemeal degranulation. *Anat. Rec. A Discov. Mol. Cell. Evol. Biol.* **270,** 103–108
26. Borges, R., Diaz-Vera, J., Dominguez, N., Arnau, M. R., and Machado, J. D. (2010) Chromogranins as regulators of exocytosis. *J. Neurochem.* **114,** 335–343
27. Kim, T., Zhang, C. F., Sun, Z., Wu, H., and Loh, Y. P. (2005) Chromogranin A deficiency in transgenic mice leads to aberrant chromaffin granule biogenesis. *J. Neurosci.* **25,** 6958–6961
28. Hendy, G. N., Li, T., Girard, M., Feldstein, R. C., Mulay, S., Desjardins, R., Day, R., Karaplis, A. C., Tremblay, M. L., and Canaff, L. (2006) Targeted ablation of the chromogranin a (Chga) gene: normal neuroendocrine dense-core secretory granules and increased expression of other granins. *Mol. Endocrinol.* **20,** 1935–1947
29. Borges, R., Travis, E. R., Hochstetler, S. E., and Wightman, R. M. (1997) Effects of external osmotic pressure on vesicular secretion from bovine adrenal medullary cells. *J. Biol. Chem.* **272,** 8325–8331
30. Glombik, M. M., and Gerdes, H. H. (2000) Signal-mediated sorting of neuropeptides and prohormones: secretory granule biogenesis revisited. *Biochimie (Paris)* **82,** 315–326
31. Taupenot, L., Harper, K. L., Mahapatra, N. R., Parmer, R. J., Mahata, S. K., and O'Connor, D. T. (2002) Identification of a novel sorting determinant for the regulated pathway in the secretory protein chromogranin A. *J. Cell Sci.* **115,** 4827–4841
32. Everse, S. J., Spraggon, G., Veerapandian, L., Riley, M., and Doolittle, R. F. (1998) Crystal structure of fragment double-D from human fibrin with two different bound ligands. *Biochemistry* **37,** 8637–8642
33. Martini, S., Consumi, M., Bonechi, C., Rossi, C., and Magnani, A. (2007) Fibrinogen-catecholamine interaction as observed by NMR and Fourier transform infrared spectroscopy. Biomacromolecules **8,** 2689–2696
34. Zhang, J. Z., and Redman, C. (1996) Fibrinogen assembly and secretion. Role of intrachain disulfide loops. *J. Biol. Chem.* **271,** 30083–30088
35. Zhang, J. Z., and Redman, C. M. (1996) Assembly and secretion of fibrinogen. Involvement of amino-terminal domains in dimer formation. *J. Biol. Chem.* **271,** 12674–12680

*Received for publication February 18, 2011.*
*Accepted for publication September 22, 2011.*